A hybrid cloud regime methodology used to evaluate Southern Ocean cloud and shortwave radiation errors in ACCESS

Shannon Mason, * Christian Jakob and Jennifer Fletcher

School of Earth, Atmosphere and Environment, Monash University, Clayton, Victoria, Australia

Charmaine Franklin

CSIRO, Aspendale, Victoria, Australia

John Haynes

Cooperative Institute for Research in the Atmosphere (CIRA), Colorado State University, CO, USA

Alain Protat

CAWCR, Bureau of Meteorology, Melbourne, Victoria, Australia

* *Corresponding author address:* School of Earth, Atmosphere and Environment, Monash University, Clayton, Victoria, Australia

E-mail: shannon.mason@monash.edu

ABSTRACT

Cloud errors in global climate models lead to significant uncertainties in climate projections; a persistent bias in many models is a deficit of shortwave cloud forcing over the Southern Ocean. To diagnose errors in cloud parameterizations we require process-oriented model evaluation methodologies; cloud regimes have been widely used in observational studies and model evaluation, but in the latter case some limitations in resolving both observed and simulated cloud behaviour.

A hybrid methodology is developed for identifying cloud regimes from observed and simulated cloud simultaneously. Eleven cloud regimes are identified in the ACCESS model for the high latitude Southern Ocean. The hybrid cloud regimes resolve the features of observed cloud as well as those characteristic of errors in the model. The simulated properties of the hybrid cloud regimes, their occurrence over the Southern Ocean and in the context of extratropical cyclones, are evaluated against observations, and their contributions to the shortwave radiation errors quantified.

Three cloud and radiation errors are identified: a deficit of cloud amount, manifest in the overprediction of a low cloud fraction regime; a tendency to produce low optical thickness versions of low and midtopped cloud regimes in the cold and dry sectors of extratropical cyclones; and an absence of shallow frontal-type cloud at the high latitudes and in the warm conveyor belt of extratropical cyclones. To address the systematic cloud property biases, the effects of changes to the model microphysics are investigated. The extended methodology is shown to resolve important features of model error in a process-oriented way, with applications to evaluating improvements in cloud parameterizations.

1. Introduction

The representation of clouds in global climate models (GCMs) is critical to modelling the Earth's radiative energy budget, atmospheric circulation and hydrological cycle, and many processes at smaller scales. Model evaluation studies consistently identify significant cloud errors (e.g. Gates et al. 1999; Zhang 2005; Trenberth and Fasullo 2010) and—while models are improving by some measures (Klein et al. 2013)—subsequent cloud feedbacks continue to be the greatest source of uncertainty in estimates of climate sensitivity (e.g. Cess et al. 1990, 1996; Colman 2003; Dufresne and Bony 2008). Many of the processes regulating cloud formation, composition and behaviour—and interactions with aerosols, radiation and dynamics—occur at scales below the resolution of GCMs, and must be parameterized. Errors related to parameterized cloud can compensate to match the bulk observations against which GCMs are tuned; for example the recurring "too few, too bright" low cloud errors in many CMIP3 models nevertheless produced near-realistic radiative fluxes (Klein et al. 2013). To identify these compensating errors and inform the improvement of parameterizations, there is a need for a "process-oriented" approach to clouds in model evaluation (Stephens 2005; Jakob 2010).

To better understand cloud processes in observations, and evaluate them in GCMs, we identify "cloud regimes"—classes of cloud with common physical characteristics and atmospheric contexts—and quantify both the physical and microphysical properties of clouds and the atmospheric processes to which they correspond. Cloud regimes can be identified from dynamical or thermodynamical parameters (see Bony and Dufresne 2005), or directly from observed cloud characteristics using a clustering algorithm to identify repeating patterns of cloud properties (e.g. Jakob and Tselioudis 2003; Jakob et al. 2005). The latter cloud regimes, also called "weather states," have proved useful in associating observed cloud properties with dynamical and thermodynamical conditions in the tropics (e.g. Rossow et al. 2005; Tan et al. 2013), extra-tropics (e.g. Gordon and Norris 2010; Haynes et al. 2011; Oreopoulos and Rossow 2011), and globally (e.g. Tselioudis et al. 2013; Oreopoulos et al. 2014).

A challenge when using cloud regimes for model evaluation is to identify cloud regimes in such a way that the representation of clouds in one or more GCMs can be compared against each other and satellite observations. There have been two approaches to identifying cloud regimes in GCMs: in the first approach (Williams and Tselioudis 2007, hereafter WT07) cloud regimes are identified from the simulated cloud properties of each GCM using the same methodology as for satellite observations. This method has the advantage of using simulated cloud directly, so that the cloud regimes accurately represent the coherent structures of cloud properties in each model. A disadvantage is that each GCM engenders a new set of cloud regimes that may be very different from those observe; without a set of cloud regimes common to model and observations, evaluation is problematic. In the WT07 approach, if simulated cloud regimes are significantly different from observations they may be subjectively grouped in to "principal" cloud regimes for evaluation. Alternatively, cloud regimes can be identified from satellite observations only, and simulated clouds assigned to cloud regimes based on average cloud properties (Williams and Webb 2009, hereafter WW09). This method has the advantage of permitting a consistent system of observed cloud regimes for evaluation and model intercomparison, and has been used in many subsequent studies (e.g. Tsushima et al. 2012; Bodas-Salcedo et al. 2012; Williams et al. 2013; Bodas-Salcedo et al. 2014). A disadvantage of the WW09 methodology is that the observed cloud regimes are not necessarily representative of the coherent structures of cloud properties in the models, so the links between cloud properties and processes are uncertain. In this paper we aim to extend these approaches by developing a hybrid methodology that retains the structures of both observed and simulated clouds. Hybrid cloud regimes are identified from both observed and simulated cloud simultaneously, ensuring the retention of observed cloud regimes to which the model must be compared, while also including the cloud structures peculiar to the model—the errors we aim to explore.

We test the utility of the hybrid cloud regime methodology by applying it to a significant cloud evaluation problem for many state-of-the-art models, the shortwave (SW) radiation biases in the high latitude Southern Ocean (50 to 65 °S) during the austral summer [December–February (DJF)]. An excess of absorbed SW radiation—associated with a deficit of cloud or cloud reflectivity in this region—was identified in the Coupled Model Intercomparison Project phase 3 (CMIP3; Trenberth and Fasullo 2010), and persists in the CMIP5 models (Li et al. 2013). Evaluations of the UK Met Office atmosphere model (Bodas-Salcedo et al. 2012) and multi-model evaluations (Williams et al. 2013) using the WW09 methodology have attributed the radiation biases to low and midtopped cloud regimes in the post-frontal and cold-air part of extratropical cyclones. Observational studies have shown that the high latitude Southern Ocean is dominated by near-ubiquitous low cloud, much of which is assigned by passive satellite observations to midtopped cloud regimes (Haynes et al. 2011; Bodas-Salcedo et al. 2014). While WW09 identify a single midtopped cloud regime in the Southern Ocean, observational studies distinguish between two midtopped cloud regimes with distinct dynamical contexts and radiative properties (Haynes et al. 2011); further evaluation of the midtopped cloud regimes at high latitudes showed that optically thick midtopped cloud regimes included both marine stratiform cloud under strongly subsiding conditions, and deeper frontal-type clouds which were associated with conditions resembling the warm conveyor belt in extratropical cyclones (Mason et al. 2014). Resolving these distinct cloud processes in model evaluation is a priority for an extended cloud regime methodology.

The GCM used in this study, the Australian Community Climate and Earth System Simulator version 1.3 (ACCESS1.3; Bi et al. 2013), exhibits SW radiation errors in the high latitude Southern Ocean during DJF typical of the persistent biases in CMIP3 and CMIP5 model intercomparisons. A first-order evaluation of ACCESS1.3 indicates a bias in SW cloud radiative effect (CRE; the difference between outgoing fluxes at TOA under clear-sky and cloudy conditions) of around 48 $\mathrm{W\,m^{-2}}$ over the high latitude Southern Ocean (Fig. 1), with a 20 % underestimate of total cloud cover (TCC) and a deficit of optically thick low- and midtopped cloud in the same region (Fig. 2; Franklin et al. 2013a).

The purpose of this study is to develop and apply an extended cloud regime methodology in an evaluation of Southern Ocean cloud and radiation errors in ACCESS1.3 in a way that links cloud properties with dynamical and microphysical cloud processes. In applying hybrid cloud regimes to the evaluation of a single GCM we evaluate the applications and limitations of the methodology for broader model evaluation and model intercomparisons. We demonstrate the use of hybrid cloud regimes to making a quantitative and process-oriented assessment of the effects of changes made to cloud parameterization in the model. The satellite observations and re-analysis data used, and the configuration of the GCM, are described in Section 2. The methodology for identifying hybrid cloud regimes for ACCESS1.3 is given in Section 3, followed by a detailed evaluation of the properties and statistics of the hybrid cloud regimes, their contribution to the SW radiation error, and their distribution in the context of a composite extratropical cyclone. An evaluation of the use of hybrid cloud regimes to quantify the effects of a modification to the model microphysics is made in Section 4. The applications and limitations of the hybrid cloud regime methodology for model evaluation are discussed in Section 5, with some concluding remarks.

2. Data

a. Passive satellite observations

The International Satellite Cloud Climatology Project (ISCCP; Rossow and Schiffer 1999) combines passive observations from geostationary and polar orbiting satellites to provide a continuous global dataset for the period July 1983 to 2009. Observations of cloud-top pressure (CTP) and cloud optical thickness (τ) are made at the scale of 1 to 5 km. The ISCCP D1 dataset consists of joint histograms of CTP-τ observations within a 280 km $\times$ 280 km equal-area grid at 3 h intervals in all day-lit areas. Top-of-atmosphere (TOA) shortwave (SW) and longwave (LW) radiative flux observations are obtained from the ISCCP FD dataset. The SW cloud radiative effect (CRE_{SW}) is the difference between the upwelling TOA radiative fluxes under clear-sky and cloudy conditions. The sign convention for TOA fluxes is such that the CRE_{SW} is negative (the cloud acts to reflect more SW radiation) and CRE_{LW} is positive (cloud inhibits LW radiation to space).

Two summers (2006 to 2008; DJF) of daily averages of ISCCP D1 and FD data were interpolated on to a regular 2.5° grid: the CTP-τ histograms were interpolated according to a nearest-neighbour interpolation scheme, and radiative fluxes using linear interpolation. In keeping with previous studies (e.g. Haynes et al. 2011; Mason et al. 2014), daily averages of 3 h ISCCP observations are used.

b. Re-Analysis

The European Centre for Medium-Range Weather Forecasting (ECMWF) interim re-analysis (ERA-Interim; Dee et al. 2011) is available at 1.5° spatial and 6 h temporal resolution. Two summers (2006 to 2008; DJF) of ERA-Interim data were re-interpolated on to a regular 2.5° grid using a linear interpolation scheme. The first and second derivatives of the ERA-Interim mean sea level pressure (MSLP) were used to identify cyclone centres as described in Field and Wood (2007). Cyclone composites are constructed by re-interpolating contemporary data on to a regular 4000 km × 4000 km grid centred at the MSLP minimum of each identified extratropical cyclone.

c. Global climate model

ACCESS1.3 is a coupled climate model developed by the Centre for Australian Weather and Climate Research (CAWCR). Its atmosphere model is based on the UK MetOffice Unified Model (UM) Global Atmosphere model version 1.0 (GA1.0; Hewitt et al. 2011). To facilitate the consistent comparison of simulated cloud with observations, the ISCCP satellite simulator (Klein and Jakob 1999; Webb et al. 2001), part of the Cloud Feedbacks Model Intercomparison Project (CFMIP) Observation Simulator Package (COSP; Bodas-Salcedo et al. 2008), is integrated in ACCESS1.3 (Franklin et al. 2013a). The ISCCP simulator output differs from ISCCP observations in that sub-visible cloud ($\tau < 0.3$) are included; however when comparing models to observations these thin clouds are ommitted as it is assumed that they would not be detected by the ISCCP cloud detection algorithms (Klein and Jakob 1999; Webb et al. 2001).

ACCESS1.3 was run in atmosphere-only mode with prescribed sea surface temperatures at N96 resolution for two years (2006 to 2008). The output fields were daily MSLP, TOA LW and SW radiative fluxes for full-sky and clear-sky conditions, and CTP-τ joint histograms from the ISCCP simulator. These data were re-interpolated on to a 2.5° grid for consistency with satellite observations and re-analysis data. MSLP and radiative fluxes were interpolated using a linear interpolation scheme, and ISCCP simulator data were interpolated using a nearest-neighbour interpolation scheme.

3. Evaluation of ACCESS1.3

a. Hybrid cloud regime methodology

In this section we extend the existing methodologies for assigning observed and simulated cloud properties to cloud regimes for model evaluation. Previous approaches have involved either clustering on the simulated cloud properties from a model (WT07)—so that the resultant cloud regimes accurately represent the model cloud behaviour, but are not necessarily comparable with observed cloud regimes—or assigning simulated clouds directly to pre-defined observed cloud regimes (WW09)—maintaining a consistent set of cloud regimes against which models can be evaluated at the risk of not necessarily resolving the cloud structures peculiar to each model. Based on the strengths and weaknesses of the existing approaches, we aim to combine the advantages of both previous method so that our extended cloud regime methodology is capable of resolving both the behaviour of the model (i.e., the repeating structures of simulated cloud properties) and the cloud regimes identified in previous observational studies.

To achieve this goal we propose clustering observed and simulated cloud properties simultaneously: the resulting clusters, called hybrid cloud regimes, represent a blend of model and observation. An individual hybrid cloud regime may consist of a mixture of observed and simulated clouds, or be made up of either mostly-observed or mostly-simulated clouds. It is worth considering what information we would expect the hybrid approach to resolve in some idealized scenarios. If the model reproduced the observations perfectly, we would expect the hybrid regimes to be identical to those from an analysis using observations alone. This applies to both the regime characteristics (as represented by the CTP-τ histogram) and its frequency of occurrence including geographic distribution. If the model was unable to reproduce any of the observed cloud regimes, we expect to find a set of regimes where some are only populated by observations and others only by model results. There would be no regime jointly populated by both and the model CTP-τ histograms would be very different from the observed. We obviously expect real model results to lie somewhere between those two extremes It is conceivable to find some observed regimes that the model simply can not represent, some model regimes that do not occur in nature, jointly populated regimes that the model can represent in principle but with the wrong frequency of occurrence or in the wrong locations, and some regimes that are well simulated. The advantages of having this comprehensive information and especially of using it to analyze model errors in other fields, such as clour radiative effects, will become apparent when we apply this technique to Southern Ocean clouds below.

Using the method for identifying cloud regimes first described in Jakob and Tselioudis (2003), we apply the k-means clustering algorithm (Anderberg 1973) to the 42-element state vectors of the CTP-τ histograms from both the ISCCP observations and from the ISCCP simulator running in ACCESS1.3 (ommitting the $\tau < 0.3$ classes for consistency with observations), using two years of austral summer (DJF) data over the region of interest (50 to 65 °S). The pool of state vectors from which the hybrid cloud regimes are identified consists of equal parts observed and simulated cloud properties, which are not differentiated by the clustering algorithm. Consistent with Haynes et al. (2011) and Mason et al. (2014), clear conditions are not removed from the data before clustering, and instances of clear skies will be included in the hybrid cloud regime with the lowest total cloud cover. Due to the ubiquity of cloud in this part of the Southern Ocean instances of completely clear conditions are rare in both observations (0.3 %) and simulations (0.06 %).

The clustering algorithm is quasi-objective in that the number of clusters must be specified. Here we require that the set of resultant hybrid cloud regimes include clusters resembling or including a set of observed cloud regimes. The number of clusters is increased until the emergent features include the expected (observed) cloud regimes, based on those previously identified for the broader Southern Ocean (30 to 65 °S; Haynes et al. 2011) and the refined analysis of midtopped cloud sub-regimes conducted for the high latitude Southern Ocean (Mason et al. 2014). We note that the emergent hybrid cloud regimes identified here are not identical to the combination of these two studies, as the cloud regimes identified in Haynes et al. (2011) include lower latitude clouds, and the cloud sub-regimes of Mason et al. (2014) were derived by clustering within previously-identified cloud regimes. However all of the features identified in the observational studies for the region of interest are represented in the hybrid cloud regimes.

Once the hybrid cloud regimes have been identified, each CTP-τ histogram (observed or simulated) is assigned to one of the cloud regimes. The assignation may be performed concurrent to the cloud regime identification, or subsequently. Assignation is determined by the least Euclidean distance between each CTP-τ joint histogram and the centroids of the cloud regimes. An alternative approach used in WW09 and subsequent studies calculates the least Euclidean distance between the total cloud cover (TCC; the sum of the joint histogram), mean cloud-top pressure ($\overline{\mathrm{CTP}}$) and mean cloud albedo ($\overline{\alpha}$; derived from τ using the ISCCP look-up table reproduced in WW09). The WW09 methodology is intended for multi-model intercomparison, wherein the mean cloud properties are a simpler requirement for participating modelling centers and using the full CTP-τ joint histograms requires a greater volume of data output and computation. While the WW09 methodology produces coherent results in many studies, we note that the differences in cloud regime frequencies of occurrence when using the two assignation methods are not negligible, especially for cloud types with complex distributions of cloud-top properties. A comparison of the two methods using the observed cloud regimes of Haynes et al. (2011) and 5 years of ISCCP D1 data between 30 to 65 °S resulted in significant differences in the frequency of occurrence ($> 10\,\%$) of some cloud regimes (not shown). In the present application to a single GCM it is practicable to use the full CTP-τ joint histograms in order to retain the structures of cloud-top properties which are indicative of sub-grid scale variability in ISCCP observations (see discussion in Mace and Wrenn 2013; Mason et al. 2014).

b. Identification and properties of hybrid cloud regimes

Eleven hybrid cloud regimes (H1–H11, ranked from high-to-low CTP and low-to-high τ) are found to be sufficient to represent the observed cloud regimes within the region of interest, as well as the emergent features of mostly-simulated cloud regimes. The CTP-τ joint histograms represent the average of all observed and simulated members of each hybrid cloud regime (Fig. 3). It is helpful to make a coarse classification by CTP level, grouping the eleven hybrid cloud regimes into boundary layer, low, midtopped and "frontal" cloud regimes. The three lowest hybrid cloud regimes (H1–H3) are predominantly boundary layer clouds representing shallow cumulus (H1) through to cumulus-stratocumulus transition clouds (H3). The low hybrid cloud regimes (H4 & H5) are associated with a range of marine stratiform clouds. The hybrid cloud regimes identified as midtopped (H6–H8) are in fact dominated by low cloud, with enough midtopped cloud to be identified as such by ISCCP retrievals (Haynes et al. 2011), and form under a range of mostly subsiding conditions (Mason et al. 2014). The frontal hybrid cloud regimes (H9–H11) include pre-frontal cirrus (H10) and deep frontal cloud (H11), as well as a shallower frontal-type cloud structure (H9). We note that, while H9 occurs at a lower CTP-level than the higher frontal cloud regimes H10 and

H11, it is displayed between the latter in the figures to save space.

By assigning each daily CTP-τ histogram to a hybrid cloud regime we derive the spatial distribution and relative frequency of occurrence (RFO) of the hybrid cloud regimes over the region of interest during DJF (Fig. 4) in both the observations and ACCESS1.3. The overall RFO of each cloud regime gives an initial indication of the hybrid cloud regimes that are modelled consistently with observations, and those that are over- and under-produced in the model.

Simulated cloud fractions are underestimated by 10 to 20 % for almost all cloud regimes, consistent with the overall deficit of TCC in ACCESS1.3. The tendency of the model to produce low cloud fractions is most apparent in the over-production of the lowest cloud fraction, lowest optical thickness cloud regime H1 throughout the area of interest (RFO of 42 % compared with 9 % observed). The CTP-τ histogram of H1 shows that this cloud regime includes a low amounts of clouds through from the surface to midlevels; we also note that the simulated spatial distribution of H1 is in areas associated not only with the observed boundary layer cloud regimes, but also with the occurrence of the midtopped cloud regime H7 in the high latitude Atlantic and Indian oceans.

ACCESS1.3 has a systematic bias toward optically thin (low-τ) low and midtopped cloud regimes. The low-τ errors appear to lead to H1 being simulated where H2 is observed (the eastern edges of the Pacific and Indian ocean basics), and the simulated distribution of H2 downstream of the Drake Passage resembles that observed of H3. A tendency to create low-τ counterparts of observed cloud regimes gives rise to low and midtopped hybrid cloud regimes H4 & H6. H4 (predominantly simulated) and H5 (predominantly observed) differ in mean cloud-top properties but correspond very closely in terms of overall RFO (15 %) and distribution in the high latitude Atlantic and central Pacific oceans. Similarly, the optically thin midtopped cloud regime H6 is simulated in the high-latitude Atlantic and Pacific oceans where H7 is observed. Corresponding to the over-prediction of these low-τ cloud regimes in ACCESS1.3, the optically thickest low and midtopped hybrid cloud regimes are very rarely simulated.

The warm frontal cloud regime H9 is almost absent in ACCESS1.3, compared with an observed RFO of 16 %, and has no clear compensating cloud regimes as identified above. As distinct from a systematic deficiency in cloud properties, this cloud error may be related to the representation of a dynamical process in the model. The higher frontal cloud regimes H10 & H11 are simulated with similar RFO to observations, but with a less cohesive distribution around the mid-latitude storm track.

An evaluation of the occurrence of the hybrid cloud regimes in the model and observations, the major cloud errors in the GCM are made explicit in a process-oriented manner. The tendency toward low TCC and low τ are manifest in additional, predominantly-simulated low and midtopped hybrid cloud regimes (H4 & H6), and the significant over-prediction of sparse (H1). While the pre-frontal cirrus (H10) and frontal (H11) hybrid cloud regimes are relatively well-represented, the shallow frontal hybrid cloud regime (H9) is almost absent from the model. We next turn our attention to identifying how these cloud errors contribute to the overall SW radiation bias.

c. Contributions to SW radiation bias

Eleven hybrid cloud regimes have been identified from passive satellite observations and simulated cloud properties in ACCESS1.3. The most significant and recurring deviations from observed cloud properties give rise to hybrid cloud regimes that are not frequently found in the observations: these preminantly-simulated hybrid cloud regimes provide an initial indication of the major cloud errors in the GCM. By associating the hybrid cloud regimes with radiation errors we can quantify the relative contributions of these major cloud errors to the total 47.6 $\mathrm{W\,m^{-2}}$ SW cloud radiative effect bias in the high latitude Southern Ocean in ACCESS1.3.

The cloud radiative effect (CRE) is the difference between clear and cloudy-sky TOA radiative fluxes. Since outgoing fluxes at TOA are defined as positive, and cloud typically has the effect of increasing reflected SW radiation, values of $\mathrm{CRE_{SW}}$ are negative. The hybrid cloud regimes with the lowest observed $\overline{\mathrm{CRE_{SW}}}$ are generally those with the optically thickest clouds and highest total cloud cover (Table 1), however the spatial distribution of the cloud regime is also important.

The mean SW cloud radiative effect bias ($\Delta\mathrm{CRE_{SW}}$) associated with each hybrid cloud regime is calculated by subtracting observed values of $\mathrm{CRE_{SW}}$ from the simulated values for the instances where each hybrid cloud regime is identified. Accordingly, positive $\Delta\mathrm{CRE_{SW}}$ indicate insufficent—or insufficiently reflective—cloud in the model, and negative biases indicate too-cloudy or too-reflective cloud errors.

The total Southern Ocean DJF $\overline{\Delta\mathrm{CRE_{SW}}}$ of $47.6\,\mathrm{W\,m^{-2}}$ can be decomposed (following WT07) into parts corresponding to errors in the cloud regime frequency of occurrence or spatial distribution (RFO errors), errors in cloud regime radiative properties (CRE errors), and a cross-term of covariant errors. The total bias is the sum of decomposed errors for all cloud regimes, such that

$$\overline{\Delta\mathrm{CRE_{SW}}} = \sum_{r=1}^{n} \underbrace{\mathrm{CRE_{SW}}_r \cdot \Delta\mathrm{RFO}_r}_{\text{RFO errors}} + \sum_{r=1}^{n} \underbrace{\Delta\mathrm{CRE_{SW}}_r \cdot \mathrm{RFO}_r}_{\text{CRE errors}} + \sum_{r=1}^{n} \underbrace{\Delta\mathrm{CRE_{SW}}_r \cdot \Delta\mathrm{RFO}_r}_{\text{cross-term}} \quad (1)$$

The decomposed $\Delta\mathrm{CRE_{SW}}$ associated with each hybrid cloud regime (Fig. 5) is dominated by RFO-related errors; this is partially a consequence of the hybrid cloud regime methodology, in which simulated clouds that are sufficiently different in their cloud-top properties from observed clouds form new clusters. This is especially true for the optically thin low and midtopped hybrid cloud regimes that are almost never observed (H4 & H6).

At each CTP level the optically thinner cloud regimes make a small or negative contribution to the $\Delta\mathrm{CRE_{SW}}$, while the optically thick hybrid cloud regimes are associated with larger positive biases. This indicates that the low-τ, low-TCC hybrid cloud regimes, which occur with similar distributions to their high-τ counterparts, partially compensate for the brighter clouds they occur in the place of. In the case of the low cloud regimes, the total error associated with the low-RFO and low $\mathrm{CRE_{SW}}$ of H5 ($23\,\mathrm{W\,m^{-2}}$) is partially compensated by the high RFO of H4 ($-13\,\mathrm{W\,m^{-2}}$); the net $\Delta\mathrm{CRE_{SW}}$ related to low cloud is $10\,\mathrm{W\,m^{-2}}$. Similarly, the over-prediction of the optically thinnest midtopped hybrid cloud regime H6 partially compensates ($-8\,\mathrm{W\,m^{-2}}$) for the low RFO of H7; the majority of the error associated with midtopped cloud ($18\,\mathrm{W\,m^{-2}}$) is related to the under-prediction and low $\mathrm{CRE_{SW}}$ of the optically thicker H8.

The strongest compensating (negative) contribution to the $\mathrm{CRE_{SW}}$ error is associated with the low-TCC, low-τ hybrid cloud regime H1. Despite being associated with the lowest observed cloud fractions and cloud brightnesses, H1 contributes $-30\,\mathrm{W\,m^{-2}}$ to the net $\mathrm{CRE_{SW}}$ error. This is due to H1 accounting for more than 40 % of the high-latitude Southern Ocean cloud in ACCESS1.3. The dominance of a low-TCC and low-τ cloud regime is symptomatic of the two key systematic biases identified in Franklin et al. (2013a).

The greatest single contributor to the net $\mathrm{CRE_{SW}}$ error is H9, the warm frontal cloud regime observed at high latitudes but hardly represented in ACCESS1.3. The deficit in the occurrence of this cloud regime is not compensated for by any optically thinner cloud regimes. The frontal cloud regimes H10 & H11 contribute around $15\,\mathrm{W\,m^{-2}}$ to the overall bias; unlike the cloud regimes at other CTP levels, the largest portion of these biases are due to CRE-related errors; the RFO-related errors may be related to the tendency in ACCESS1.3 toward a less coherent band of frontal cloud at lower latitudes.

d. Dynamical contexts of the hybrid cloud regimes

We have used hybrid cloud regimes to identify the major shortcomings in the simulation of clouds in the high latitude Southern Ocean in ACCESS1.3, and quantified their contributions to the SW radiation errors. It remains to investigate if the hybrid cloud regimes are associated with consistent dynamical and thermodynamical processes. In observational studies it is common to characterize cloud regimes by their contemporary meteorology derived from re-analyses (e.g. Gordon and Norris 2010; Haynes et al. 2011; Mason et al. 2014). This approach should be well-suited to GCMs, wherein these fields are directly available, however direct comparisons of dynamical fields in GCMs and re-analysis are frustrated by possible errors in model dynamics. An alternative approach is to consider cloud regimes in the context of a composite extratropical cyclone, the structure of which is both well understood in terms of observed dynamical, thermodynamical and cloud processes, and resolved by climate models (Catto et al. 2010). A evaluation of Southern Hemisphere extratropical cyclones in an earlier version of the ACCESS model modified to use the same cloud scheme as ACCESS1.3 (Govekar et al. 2014) found that the circulation and dynamical variables were significantly weaker than in re-analyses, and showed that the deficits of low cloud in this context are consistent with the broader evaluation of clouds in ACCESS1.3 (Franklin et al. 2013a) and with evaluations of extratropical cyclones in other models. Extratropical cyclones are the dominant synoptic scale feature in the high latitude Southern Ocean in terms of both cloud and precipitation (Bodas-Salcedo et al. 2014; Papritz et al. 2014), and cloud regimes have been used effectively to evaluate cloud in this context (e.g. Bodas-Salcedo et al. 2012, 2014). However, we note that not all cloud processes relevant to the high latitude Southern Ocean are necessarily represented within the dynamics of the composite extratropical cyclone. The cloud processes associated with anti-cyclones, warm ridges and mesoscale cyclones ("polar lows")—and their representation in climate models—are of considerable interest for model evaluation, but are not considered here.

We identify extratropical cyclones in observations and simulations as described in Field and Wood (2007) using MSLP from ERA-Interim re-analysis to identify cyclone centres contemporary to the satellite observations. Cloud regime occurrence and TOA radiative flux fields from observations and ACCESS1.3 are re-interpolated on to a 2000 km × 2000 km grid centred at each MSLP minimum, and candidates are filtered to select only cyclones centred from 50 to 65 °S.

The observed RFOs of the hybrid cloud regimes in the context of the composite cyclone (Fig. 6) agree well with other composite cyclone studies. We note that the multiple mid-topped cloud regimes identified in this study are found in separate and coherent parts of the extratropical cyclone: this reinforces the distinction between optically thin and optically thick midtopped, and shallow frontal cloud regimes made in Mason et al. (2014). The profiles of dynamical and thermodynamical properties from re-analysis (not shown) are consistent with those presented in previous studies (e.g. Gordon and Norris 2010; Haynes et al. 2011; Mason et al. 2014). The warm sector of the composite extratropical cyclone is characterized by the occurrence of the frontal cirrus (H10) and deep frontal (H11) cloud regimes. H10 is observed further from the cyclone centre and appears to be associated with both pre-frontal cirrus and other high and thin cloud in other contexts. H11 is found along the cold front, under conditions of strong ascent. H9 occurs predominantly near the cyclone center and into the cold sector, and resembles the warm conveyor belt (WCB) flow which overshoots the warm front; we note that a similar midtopped cloud sub-regime identified in Mason et al. (2014) was associated with conditions resembling that of the WCB. The warm sector is also associated with the shallow cloud regime H3. The cold sector of the extratropical cyclone consists of easterly flow ahead of the warm front turning equatorward behind the storm centre, where it meets the descending dry sector. The cold sector is dominated by low and midtopped stratiform cloud regimes H5 and H8, which form under subsiding conditions ahead of the warm front. These stratiform clouds transition to H7 in the post-frontal region of cold-air advection, and finally in the driest section the shallow cumulus (H2) dominates.

The ACCESS1.3 cloud errors in the context of the extratropical cyclone are consistent with those identified so far. The frontal cloud regime H11 is found closest to the storm centre: the shallow frontal cloud regime H9 is not present near the warm front, while the optically thinner H10 is found throughout much of the inner warm sector. The compensating relationships between predominantly-simulated and predominantly observed hybrid cloud regimes are evident in the cold and dry sectors, indicating the consistent low-τ and low TCC biases. Where H3 is observed in the warm sector, its low-τ counterpart H2 is simulated. The cold sector is dominated by the low-τ and low-TCC biases: H4 and H6 are simulated through the cold sector and wrapping around the storm centre, while the dry sector is dominated by low TCC cloud (H1).

The occurrence of the hybrid cloud regimes in the context of the extratropical cyclone illustrate consistent relationships between cloud properties and dynamical and thermodynamical conditions in both the observations and the model, reinforcing the spatial distributions of the cloud regimes over coherent parts of the high latitude Southern Ocean. In both the composite cyclones and Southern Ocean maps the significant over-production of the low-TCC cloud regime H1, and the compensation of low-τ cloud regimes H2, H4 and H6 for their higher-τ counterparts, are evident. These over-predicted cloud regimes make negative contributions to the SW radiation errors, but only partially compensate for the lack of brighter clouds. The single largest contributor to the SW radiation bias in ACCESS1.3 is the near-absence of the shallow frontal cloud regime H9 at the high latitudes and at the centre of the extratropical cyclone.

4. Evaluation of parameterization changes

We have used the hybrid cloud regimes to identify three major high latitude Southern Ocean cloud and radiation errors in ACCESS1.3. The model is characterised by systematic deficits of total cloud cover and cloud optical thickness affecting low and midtopped cloud, especially in the cold and dry sectors of extratropical cyclones. The systematic bias toward low-τ cloud suggests that errors relating to microphysical parameterizations affect the radiative properties of clouds. Such parameters may include cloud thermodynamic phase, droplet size and concentration, and properties such as total cloud amount or cloud lifetime which are affected by precipitation rates and mixing with dry air. To target the optical thickness biases we make three changes to the representation of clouds intended to reduce the Southern Ocean cloud and radiative biases in ACCESS1.3. A new autoconversion scheme (Franklin 2008) is implemented, as it was shown by Franklin et al. (2013b) to increase the occurrence of optically thicker low clouds and reduce the overestimate of drizzle in tropical boundary layer clouds. Franklin et al. (2013a) demonstrated that by reducing the fall speed of the ice aggregate category in the model the occurrence of optically thicker low-midlevel clouds was increased over the Southern Ocean. In this study these fall speeds are reduced by one third. An additional change is made to the erosion timescale parameter that controls the rate at which the liquid cloud fraction is reduced by the mixing of cloudy air with drier environmental air. This parameter takes the value of $-4.5 \times 10^{-5}\,\mathrm{s}^{-1}$ in the control version of ACCESS1.3 and is reduced by half in the modified cloud parameterizations experiment. While this change directly affects the cloud fraction, it indirectly affects the microphysical processes by changing the in-cloud water contents that are used in the microphysical parameterisations such as the autoconversion scheme. Testing these three changes independently shows that the largest change in both the ISCCP diagnostics and the cloud radiative effects comes from the different autoconversion scheme (not shown). The other two cloud changes also positively affect the radiative properties of the clouds over the Southern Ocean; the combined set of these three changes produces the lowest shortwave cloud radiative effect bias, and is used in this study.

ACCESS1.3 was run in atmosphere-only mode with the modified cloud microphysics in the same way as for the initial model evaluation. Two years of DJF data, including CTP-τ histograms from the ISCCP simulator, MSLP, and TOA radiative fluxes, are processed as described earlier. Instead of generating a new set of hybrid cloud regimes, the CTP-τ histograms are assigned to the cloud regimes derived from the standard ACCESS1.3 model; the differences in the RFO and $\mathrm{CRE_{SW}}$ can be compared directly, or summarized according to their contribution to the $\Delta\mathrm{CRE_{SW}}$.

The decomposed $\mathrm{CRE_{SW}}$ bias (Fig. 7) summarizes the effects of the modified microphysics on the radiation errors in ACCESS1.3. The overall effect is a $10\,\mathrm{W\,m^{-2}}$ reduction in the total $\mathrm{CRE_{SW}}$ bias. The majority of this improvement is due to a systematic increase of τ across all hybrid cloud regimes: the $\mathrm{CRE_{SW}}$-related component of the error for each cloud regime decreases by as much as $2.0\,\mathrm{W\,m^{-2}}$, including a worsening of the negative errors associated with the optically thin hybrid cloud regimes (H1, H2 & H4), which act to compensate for the absent optically thicker cloud regimes.

Where the changes in the optical properties of a cloud regime are large enough, instances of cloud previously belonging to one hybrid cloud regime may be assigned to an optically thicker hybrid cloud regime. These changes in cloud regime assignations lead to changes in the RFO-related error of both the prior and subsequent cloud regime: this is most apparent in the compensating RFO-related errors associated with the optically thin midtopped hybrid cloud regimes H6 & H7—each is reduced in magnitude by around $5\,\mathrm{W\,m^{-2}}$, and the net bias associated with midtopped cloud overall is largely unchanged. The RFO of H1 decreases in a similar manner, corresponding to a $3\,\mathrm{W\,m^{-2}}$ improvement in the RFO-related bias—a net increase in the overall $\mathrm{CRE_{SW}}$ error, since H1 compensates for the lack of optically thicker cloud regimes. Reductions of total bias associated with the frontal cloud regimes H10 & H11 are partly due to increased τ, and partly due to increased RFO of both cloud regimes, particularly H11.

The effect of the cloud microphysics changes was to reduce the systematic deficit of cloud optical thickness across all cloud regimes. This shift in cloud properties leads to reduced frequencies of occurrence of the optically thinnest cloud regimes (H1 & H6) and higher mean optical thickness within cloud regimes, with the greatest net effect being a reduction of errors associated with low and frontal clouds of around $4\,\mathrm{W\,m^{-2}}$. Equal and opposite improvements in the RFO-related errors of two midtopped hybrid cloud regimes were due to a shift toward optically thicker cloud; this reduced the compensation of one mostly-simulated cloud regime for a mostly-observed one, but did not reduce the net radiative bias. In several cases the increase in cloud brightness worsened the $\mathrm{CRE_{SW}}$ bias (H2 & H4), or had little effect (H8 & H9). That these microphysics changes had no effect on the single largest source of SW cloud errors in ACCESS1.3 illustrates the strength of the hybrid cloud regime approach—an improved understanding of the effects of model changes on individual cloud regimes.

5. Discussion and conclusions

We have presented a hybrid methodology for identifying cloud regimes from satellite observations and model-simulated cloud properties simultaneously. This approach expands on previous methodologies for identifying cloud regimes for model evaluation, with the advantage that the cloud regimes include a fixed reference to the observed cloud properties against which the models are evaluated, while also permitting cloud regimes that are peculiar to the model. The emergent hybrid cloud regimes include pairs of cloud regimes with similar spatial distributions and dynamical contexts, where one hybrid cloud regime is predominantly simulated and the other is predominantly observed; the differences between these pairs of hybrid cloud regimes relate to the major cloud property errors in the GCM.

Based on two DJFs of simulated and observed cloud data, we identified eleven hybrid cloud regimes with which to evaluate high latitude Southern Ocean clouds in ACCESS1.3. We identified three major sources of cloud and radiation errors, and described the dynamical context of these cloud regimes as inferred from composite extratropical cyclones. Consistent with Franklin et al. (2013a), total cloud cover in ACCESS1.3 is consistently under-predicted, which contributes to the weak SW forcing of most cloud regimes; compensating for the low total cloud fraction in the other cloud regimes, the cloud regime associated with lower cloud amounts is strongly over-predicted, especially in the cold and dry sectors of extratropical cyclones and throughout the high latitude Southern Ocean; while the SW cloud radiative effect of this cloud regime is relatively weak, its vast over-prediction has a strong compensating effect, making a $-30\,\mathrm{W\,m^{-2}}$ contribution to the overall SW bias.

Low cloud optical thickness biases in ACCESS1.3 were found across almost all hybrid cloud regimes. In some cases this is manifest in additional low and midtopped hybrid cloud regimes that are simulated in place of optically thicker observed counterparts, especially in the cold and dry sectors of extratropical cyclones. These partially compensate for optically thicker cloud regimes not well-represented in the model.

The low optical thickness errors were mitigated by around $10\,\mathrm{W\,m^{-2}}$ by implementing a series of microphysics changes. The result was a systematic increase in cloud albedo across all simulated cloud, which had the greatest net improvement on the SW forcing errors of the low and frontal cloud regimes. Changing the cloud microphysics to systematically increase cloud albedo may constitute part of an improvement to the Southern Ocean cloud and radiation biases identified in ACCESS1.3, but in this case was not sufficient to address some of the largest deficits in the optical thickness of stratiform clouds.

The largest contributor to the SW radiation bias over the Southern Ocean is the shallow frontal cloud regime observed at high latitudes and in the warm fronts of extratropical cyclones; these clouds were very rarely identified in the model, and a compensating relationship with an optically thinner cloud regime was not identified. The other frontal cloud regimes are generally too optically thin also; the cirrus cloud regime is simulated too frequently, and the frontal cloud regime not frequently enough.

In this study the cloud regimes were linked to dynamical processes in the context of extratropical cyclones. Considering the Southern Ocean cloud regimes only in the context of extratropical cyclones is not necessarily representative: for example, while shallow or warm-frontal cloud makes the largest net contribution to the SW bias, the warm front does not correspond to the region of greatest SW bias in the context of the composite extratropical cyclone—the cold and dry sectors (e.g. Bodas-Salcedo et al. 2012, 2014) where errors in total cloud cover and optical thickness dominate, and where modifications to the boundary-layer scheme have had some success in mitigating the total error (Bodas-Salcedo et al. 2012). Nevertheless the magnitude of the bias associated with the shallow or warm frontal cloud suggests it is not simulated well. Case studies will be required to better understand the causes for this model behaviour.

The approach of identifying pairs of mostly-simulated and mostl-observed hybrid cloud regimes has proved useful: the pairs were shown to be simulated with similar spatial distributions to their observed counterparts, and these relationships were also found in the dynamical context of a composite extratropical cyclone. However more work could be done to quantify the association between processes in the model and observations more directly, perhaps by using the model in hindcast mode to evaluate case studies.

The hybrid cloud regimes are identified for a single GCM, and further work would be required to use this approach for the evaluation of multiple models. However the hybrid cloud regimes provide a fixed reference to cloud errors identified in a GCM, making this a promising tool for quantifying the effects of changes to the model on the properties and statistics of the hybrid cloud regimes.

While the Southern Ocean SW radiation errors in ACCESS1.3 are representative of radiation biases in many state-of-the-art models, the nature and causes of these biases are almost certainly not the same in each model.

Acknowledgments.

This research has been supported by ARC Discovery and Linkage Grant Schemes (DP130100869 and LP0883961) as well as the ARC Centre of Excellence for Climate System Science (CE110001028). We thank Alejandro Bodas-Salcedo and Keith Williams at the UK Met Office for their generous cooperation and feedback.

REFERENCES

Anderberg, M., 1973: Cluster analysis for applications. Ph.D. thesis, Academic Press, 359 pp., New York, NY, USA, URL http://cdsweb.cern.ch/record/103120.

Bi, D., et al., 2013: The ACCESS coupled model: description, control climate and evaluation. *Aust. Meteorol. Oceanogr. J*, **63 (1)**, 41–64, URL http://climate-cms.unsw.wikispaces.net/file/view/Bi_AMOJ_ACCESS-CM_revision.pdf.

Bodas-Salcedo, A., M. J. Webb, M. E. Brooks, M. A. Ringer, K. D. Williams, S. F. Milton, and D. R. Wilson, 2008: Evaluating cloud systems in the Met Office global forecast model using simulated CloudSat radar reflectivities. *Journal of Geophysical Research*, **113**, doi:10.1029/2007JD009620, URL http://www.agu.org/pubs/crossref/2008/2007JD009620.shtml.

Bodas-Salcedo, A., K. D. Williams, P. R. Field, and A. P. Lock, 2012: The surface downwelling solar radiation surplus over the Southern Ocean in the Met Office model: the role of midlatitude cyclone clouds. *Journal of Climate*, 120521141256006, doi:10.1175/JCLI-D-11-00702.1, URL http://journals.ametsoc.org/doi/abs/10.1175/JCLI-D-11-00702.1.

Bodas-Salcedo, A., et al., 2014: Origins of the Solar Radiation Biases over the Southern Ocean in CFMIP2 Models*. *Journal of Climate*, **27 (1)**, 41–56, doi:10.1175/JCLI-D-13-00169.1, URL http://journals.ametsoc.org/doi/pdf/10.1175/JCLI-D-13-00169.1http://journals.ametsoc.org/doi/abs/10.1175/JCLI-D-13-00169.1.

Bony, S. and J.-L. Dufresne, 2005: Marine boundary layer clouds at the heart of tropical cloud feedback uncertainties in climate models. *Geophysical Research Letters*, **32 (20)**, L20 806, URL http://www.lmd.jussieu.fr/$\sim$jldufres/publi/2005/Bony.Dufresne-grl-2005.pdfhttp://www.agu.org/pubs/crossref/2005/2005GL023851.shtml.

Catto, J. L., L. C. Shaffrey, and K. I. Hodges, 2010: Can climate models capture the structure of extratropical cyclones? *Journal of Climate*, **23 (7)**, 1621–1635, URL http://journals.ametsoc.org/doi/abs/10.1175/2009JCLI3318.1http://journals.ametsoc.org/action/cookieAbsent.

Cess, R., et al., 1990: Intercomparison and interpretation of climate feedback processes in 19 atmospheric general circulation models. *Journal of Geophysical Research*, **95 (16)**, 601 216, URL http://kiwi.atmos.colostate.edu/pubs/Cessetal-1990.pdf.

Cess, R. D., et al., 1996: Cloud feedback in atmospheric general circulation models: An update. *Journal of Geophysical Research*, **101 (D8)**, 12 791, doi:10.1029/96JD00822, URL http://onlinelibrary.wiley.com/doi/10.1029/96JD00822/fullhttp://doi.wiley.com/10.1029/96JD00822.

Colman, R., 2003: A comparison of climate feedbacks in general circulation models. *Climate Dynamics*, **20 (7-8)**, 865–873, doi:10.1007/s00382-003-0310-z, URL http://link.springer.com/article/10.1007/s00382-003-0310-z.

Dee, D. P., et al., 2011: The ERAInterim reanalysis: configuration and performance of the data assimilation system. *Quarterly Journal of the Royal Meteorological Society*, **137 (656)**, 553–597, doi:10.1002/qj.828, URL http://onlinelibrary.wiley.com/doi/10.1002/qj.828/abstracthttp://onlinelibrary.wiley.com/store/10.1002/qj.828/asset/828_ftp.pdf?v=1&t=gyxlxmk4&s=e5a6ee75aca880d742d85db223352f476cd1a8b0.

Dufresne, J.-L. and S. Bony, 2008: An Assessment of the Primary Sources of Spread of Global Warming Estimates from Coupled AtmosphereOcean Models. *Journal of Climate*,

21 (19), 5135–5144, doi:10.1175/2008JCLI2239.1, URL http://journals.ametsoc.org/doi/abs/10.1175/2008JCLI2239.1.

Field, P. R. and R. Wood, 2007: Precipitation and Cloud Structure in Midlatitude Cyclones. *Journal of Climate*, **20 (2)**, 233–254, doi:10.1175/JCLI3998.1, URL http://journals.ametsoc.org/doi/abs/10.1175/JCLI3998.1http://envsci.rutgers.edu/$\sim$toine379/extremeprecip/papers/field_and_wood_2007.pdf.

Franklin, C. N., 2008: A Warm Rain Microphysics Parameterization that Includes the Effect of Turbulence. *Journal of the Atmospheric Sciences*, **65 (6)**, 1795–1816, doi:10.1175/2007JAS2556.1, URL http://journals.ametsoc.org/doi/abs/10.1175/2007JAS2556.1.

Franklin, C. N., Z. Sun, D. Bi, M. Dix, H. Yan, and A. Bodas-Salcedo, 2013a: Evaluation of clouds in ACCESS using the satellite simulator package COSP: Global, seasonal, and regional cloud properties: EVALUATION OF CLOUDS IN ACCESS1.3. *Journal of Geophysical Research: Atmospheres*, **118 (2)**, 732–748, doi:10.1029/2012JD018469, URL http://doi.wiley.com/10.1029/2012JD018469.

Franklin, C. N., Z. Sun, D. Bi, M. Dix, H. Yan, and A. Bodas-Salcedo, 2013b: Evaluation of clouds in ACCESS using the satellite simulator package COSP: Regime-sorted tropical cloud properties. *Journal of Geophysical Research: Atmospheres*, **118 (12)**, 6663–6679, doi:10.1002/jgrd.50496, URL http://onlinelibrary.wiley.com/doi/10.1002/jgrd.50496/fullhttp://doi.wiley.com/10.1002/jgrd.50496.

Gates, W. L., et al., 1999: An overview of the results of the Atmospheric Model Intercomparison Project (AMIP I). *Bulletin of the American Meteorological Society*, **80 (1)**, 29–55, URL http://journals.ametsoc.org/doi/abs/10.1175/1520-0477(1999)080%3C0029:AOOTRO%3E2.0.CO;2http://www.phy.pku.edu.cn/climate/class/cm2010/amip-BAMS-1999.pdf.

Gordon, N. and J. Norris, 2010: Cluster analysis of midlatitude oceanic cloud regimes: mean properties and temperature sensitivity. *Atmospheric Chemistry and Physics*, **10 (13)**, 6435–6459, URL http://www.atmos-chem-phys.net/10/6435/2010/acp-10-6435-2010.pdf.

Govekar, P. D., C. Jakob, and J. Catto, 2014: The relationship between clouds and dynamics in Southern Hemisphere extratropical cyclones in the real world and a climate model. *Journal of Geophysical Research: Atmospheres*, 2013JD020699, doi:10.1002/2013JD020699, URL http://onlinelibrary.wiley.com/doi/10.1002/2013JD020699/abstract.

Haynes, J. M., C. Jakob, W. B. Rossow, G. Tselioudis, and J. R. Brown, 2011: Major Characteristics of Southern Ocean Cloud Regimes and Their Effects on the Energy Budget. *Journal of Climate*, **24 (19)**, 5061–5080, doi:10.1175/2011JCLI4052.1, URL http://journals.ametsoc.org/doi/abs/10.1175/2011JCLI4052.1http://pubs.giss.nasa.gov/abs/ha04510h.html.

Hewitt, H. T., D. Copsey, I. D. Culverwell, C. M. Harris, R. S. R. Hill, A. B. Keen, A. J. McLaren, and E. C. Hunke, 2011: Design and implementation of the infrastructure of HadGEM3: The next-generation Met Office climate modelling system. *Geoscientific Model Development*, **4 (2)**, 223–253, URL http://www.geosci-model-dev.net/4/223/2011/gmd-4-223-2011.htmlhttp://www.geosci-model-dev.net/4/223/2011/gmd-4-223-2011.pdf.

Jakob, C., 2010: Accelerating Progress in Global Atmospheric Model Development through Improved Parameterizations: Challenges, Opportunities, and Strategies. *Bulletin of the American Meteorological Society*, **91 (7)**, 869–875, doi:10.1175/2009BAMS2898.1, URL http://journals.ametsoc.org/doi/abs/10.1175/2009BAMS2898.1http://journals.ametsoc.org/doi/pdf/10.1175/2009BAMS2898.1.

Jakob, C. and G. Tselioudis, 2003: Objective identification of cloud regimes in the Tropical

Western Pacific. *Geophysical Research Letters*, **30 (21)**, 2082, doi:10.1029/2003GL018367, URL http://www.agu.org/pubs/crossref/2003/2003GL018367.shtml.

Jakob, C., G. Tselioudis, and T. Hume, 2005: The Radiative, Cloud, and Thermodynamic Properties of the Major Tropical Western Pacific Cloud Regimes. *Journal of Climate*, **18 (8)**, 1203–1215, doi:10.1175/JCLI3326.1, URL http://users.monash.edu.au/$\sim$cjakob/Papers/jakob_etal_jcl2005.pdfhttp://journals.ametsoc.org/doi/pdf/10.1175/JCLI3326.1http://journals.ametsoc.org/doi/abs/10.1175/JCLI3326.1.

Klein, S. A. and C. Jakob, 1999: Validation and Sensitivities of Frontal Clouds Simulated by the ECMWF Model. *Monthly Weather Review*, **127 (10)**, 2514–2531, doi:10.1175/1520-0493(1999)127⟨2514:VASOFC⟩2.0.CO;2, URL http://journals.ametsoc.org/doi/full/10.1175/1520-0493(1999)127<2514:VASOFC>2.0.CO;2http://journals.ametsoc.org/doi/abs/10.1175/1520-0493(1999)127<2514:VASOFC>2.0.CO;2.

Klein, S. A., Y. Zhang, M. D. Zelinka, R. Pincus, J. Boyle, and P. J. Gleckler, 2013: Are climate model simulations of clouds improving? An evaluation using the ISCCP simulator. *Journal of Geophysical Research: Atmospheres*, **118 (3)**, 1329–1342, doi:10.1002/jgrd.50141, URL http://onlinelibrary.wiley.com/doi/10.1002/jgrd.50141/abstracthttp://onlinelibrary.wiley.com/doi/10.1002/jgrd.50141/full.

Li, J.-L. F., D. E. Waliser, G. Stephens, S. Lee, T. L'Ecuyer, S. Kato, N. Loeb, and H.-Y. Ma, 2013: Characterizing and understanding radiation budget biases in CMIP3/CMIP5 GCMs, contemporary GCM, and reanalysis. *Journal of Geophysical Research: Atmospheres*, **118 (15)**, 8166–8184, doi:10.1002/jgrd.50378, URL http://onlinelibrary.wiley.com/doi/10.1002/jgrd.50378/abstracthttp://doi.wiley.com/10.1002/jgrd.50378.

Mace, G. G. and F. J. Wrenn, 2013: Evaluation of the Hydrometeor Layers in the East and West Pacific within ISCCP Cloud-Top PressureOptical Depth Bins Using Merged CloudSat and CALIPSO Data. *Journal of Climate*, **26 (23)**, 9429–9444, doi:10.1175/JCLI-D-12-00207.1, URL http://journals.ametsoc.org/doi/abs/10.1175/JCLI-D-12-00207.1.

Mason, S., C. Jakob, A. Protat, and J. Delanoë, 2014: Characterizing Observed Midtopped Cloud Regimes Associated with Southern Ocean Shortwave Radiation Biases. *Journal of Climate*, **27 (16)**, 6189–6203, doi:10.1175/JCLI-D-14-00139.1, URL http://journals.ametsoc.org/doi/abs/10.1175/JCLI-D-14-00139.1.

Oreopoulos, L., N. Cho, D. Lee, S. Kato, and G. J. Huffman, 2014: An examination of the nature of global MODIS cloud regimes. *Journal of Geophysical Research: Atmospheres*, **119 (13)**, 8362–8383, doi:10.1002/2013JD021409, URL http://onlinelibrary.wiley.com/doi/10.1002/2013JD021409/abstracthttp://doi.wiley.com/10.1002/2013JD021409.

Oreopoulos, L. and W. B. Rossow, 2011: The cloud radiative effects of International Satellite Cloud Climatology Project weather states. *Journal of Geophysical Research*, **116**, 22 PP., doi:201110.1029/2010JD015472, URL http://www.agu.org/pubs/crossref/2011/2010JD015472.shtml.

Papritz, L., S. Pfahl, I. Rudeva, I. Simmonds, H. Sodemann, and H. Wernli, 2014: The Role of Extratropical Cyclones and Fronts for Southern Ocean Freshwater Fluxes. *Journal of Climate*, **27 (16)**, 6205–6224, doi:10.1175/JCLI-D-13-00409.1, URL http://journals.ametsoc.org/doi/abs/10.1175/JCLI-D-13-00409.1http://journals.ametsoc.org/doi/pdf/10.1175/JCLI-D-13-00409.1.

Rossow, W. and R. Schiffer, 1999: Advances in understanding clouds from ISCCP. *Bulletin* of the American Meteorological Society*, **80**, 2261–2288, URL http://nml.yonsei.ac.kr/front/bbs/paper/bams/BAMS_1999-18_Rossow_and_Schiffer.pdf.

Rossow, W., G. Tselioudis, A. Polak, and C. Jakob, 2005: Tropical climate described as a distribution of weather states indicated by distinct mesoscale cloud property mixtures. *Geophys. Res. Lett*, **32**, L21 812.

Stephens, G. L., 2005: Cloud feedbacks in the climate system: A critical review. *Journal of climate*, **18 (2)**, 237–273, URL http://journals.ametsoc.org/doi/abs/10.1175/JCLI-3243.1http://climateknowledge.org/figures/Rood_Climate_Change_AOSS480_Documents/QC013_Stephens_Cloud_Feedback_JClim_2005.pdf.

Tan, J., C. Jakob, and T. P. Lane, 2013: On the Identification of the Large-Scale Properties of Tropical Convection Using Cloud Regimes. *Journal of Climate*, **26 (17)**, 6618–6632, doi:10.1175/JCLI-D-12-00624.1, URL http://journals.ametsoc.org/doi/abs/10.1175/JCLI-D-12-00624.1.

Trenberth, K. and J. T. Fasullo, 2010: Simulation of present-day and twenty-first-century energy budgets of the southern oceans. *Journal of Climate*, **23 (2)**, 440–454, doi:10.1175/2009JCLI3152.1.

Tselioudis, G., W. Rossow, Y. Zhang, and D. Konsta, 2013: Global Weather States and Their Properties from Passive and Active Satellite Cloud Retrievals. *Journal of Climate*, **26 (19)**, 7734–7746, doi:10.1175/JCLI-D-13-00024.1, URL http://www.knmi.nl/samenw/euclipse/Publications/Tselioudis_Rossow_Zhang_Konsta_Global_Weather_States_and_their_Properties_from_Passive_and_Active_Satellite_Cloud_Retrievals.pdfhttp://journals.ametsoc.org/doi/abs/10.1175/JCLI-D-13-00024.1.

Tsushima, Y., M. A. Ringer, M. J. Webb, and K. D. Williams, 2012: Quantitative evaluation of the seasonal variations in climate model cloud regimes.

Climate Dynamics, **41 (9-10)**, 2679–2696, doi:10.1007/s00382-012-1609-4, URL http://link.springer.com/article/10.1007/s00382-012-1609-4http://link.springer.com/10.1007/s00382-012-1609-4http://link.springer.com/content/pdf/10.1007/s00382-012-1609-4.

Webb, M. J., C. Senior, S. Bony, and J. Morcrette, 2001: Combining ERBE and ISCCP data to assess clouds in the Hadley Centre, ECMWF and LMD atmospheric climate models. *Climate Dynamics*, **17 (12)**, 905–922.

Williams, K. D. and G. Tselioudis, 2007: GCM intercomparison of global cloud regimes: present-day evaluation and climate change response. *Climate Dynamics*, **29 (2-3)**, 231–250, doi:10.1007/s00382-007-0232-2, URL http://www.springerlink.com/index/10.1007/s00382-007-0232-2.

Williams, K. D. and M. J. Webb, 2009: A quantitative performance assessment of cloud regimes in climate models. *Climate Dynamics*, **33 (1)**, 141–157, doi:10.1007/s00382-008-0443-1, URL http://www.springerlink.com/index/10.1007/s00382-008-0443-1.

Williams, K. D., et al., 2013: The Transpose-AMIP II Experiment and Its Application to the Understanding of Southern Ocean Cloud Biases in Climate Models. *Journal of Climate*, **26 (10)**, 3258–3274, doi:10.1175/JCLI-D-12-00429.1, URL http://users.monash.edu.au/$\sim$cjakob/Papers/williams_etal_jcl2012.pdfhttp://journals.ametsoc.org/doi/abs/10.1175/JCLI-D-12-00429.1.

Zhang, M. H., 2005: Comparing clouds and their seasonal variations in 10 atmospheric general circulation models with satellite measurements. *Journal of Geophysical Research*, **110 (D15)**, D15S02, doi:10.1029/2004JD005021, URL http://www.gfdl.noaa.gov/bibliography/related_files/mhz0501.pdfhttp:

//www.agu.org/pubs/crossref/2005/2004JD005021.shtmlhttp://doi.wiley.com/10.1029/2004JD005021.

List of Tables

Table 1. The observed and simulated properties of the hybrid cloud regimes

CTP class	Cloud regime	TCC [%]		RFO [%]		$\overline{\mathrm{CRE}_{\mathrm{SW}}}$ [W m^{-2}]	
		obs	sim	obs	sim	obs	sim
Boundary layer	H1	63.0	42.8	8.9	41.8	−76.8	−88.0
	H2	74.6	71.6	7.1	11.5	−86.0	−104.2
	H3	91.9	79.7	9.1	0.1	−149.6	−124.4
Low	H4	85.5	72.6	2.1	15.4	−101.8	−103.4
	H5	93.9	76.2	15.1	0.4	−154.8	−120.9
Midtopped	H6	89.7	66.4	0.2	8.5	−96.3	−95.7
	H7	89.5	73.6	14.2	6.6	−116.0	−99.6
	H8	95.1	74.6	10.5	0.1	−159.8	−111.5
Frontal	H9	96.4	76.5	16.9	0.5	−171.8	−95.4
	H10	93.3	73.6	8.9	10.7	−140.1	−87.4
	H11	97.2	75.0	6.9	4.3	−194.0	−91.2

List of Figures

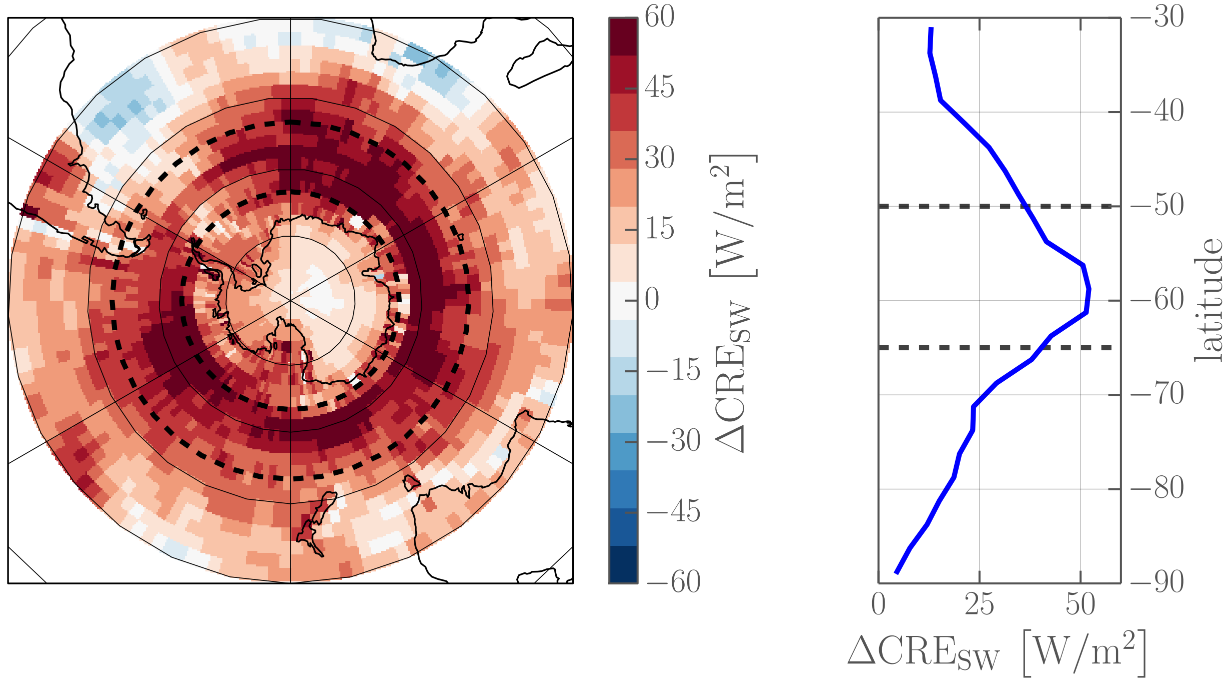

FIG. 1. Map of the CRE_{SW} bias in ACCESS1.3 with respect to ISCCP-FD passive satellite observations over the southern hemisphere extra-tropics (left), and the zonal mean bias (right). The high latitude Southern Ocean region (50 to 65 °S) is indicated with thick lines.

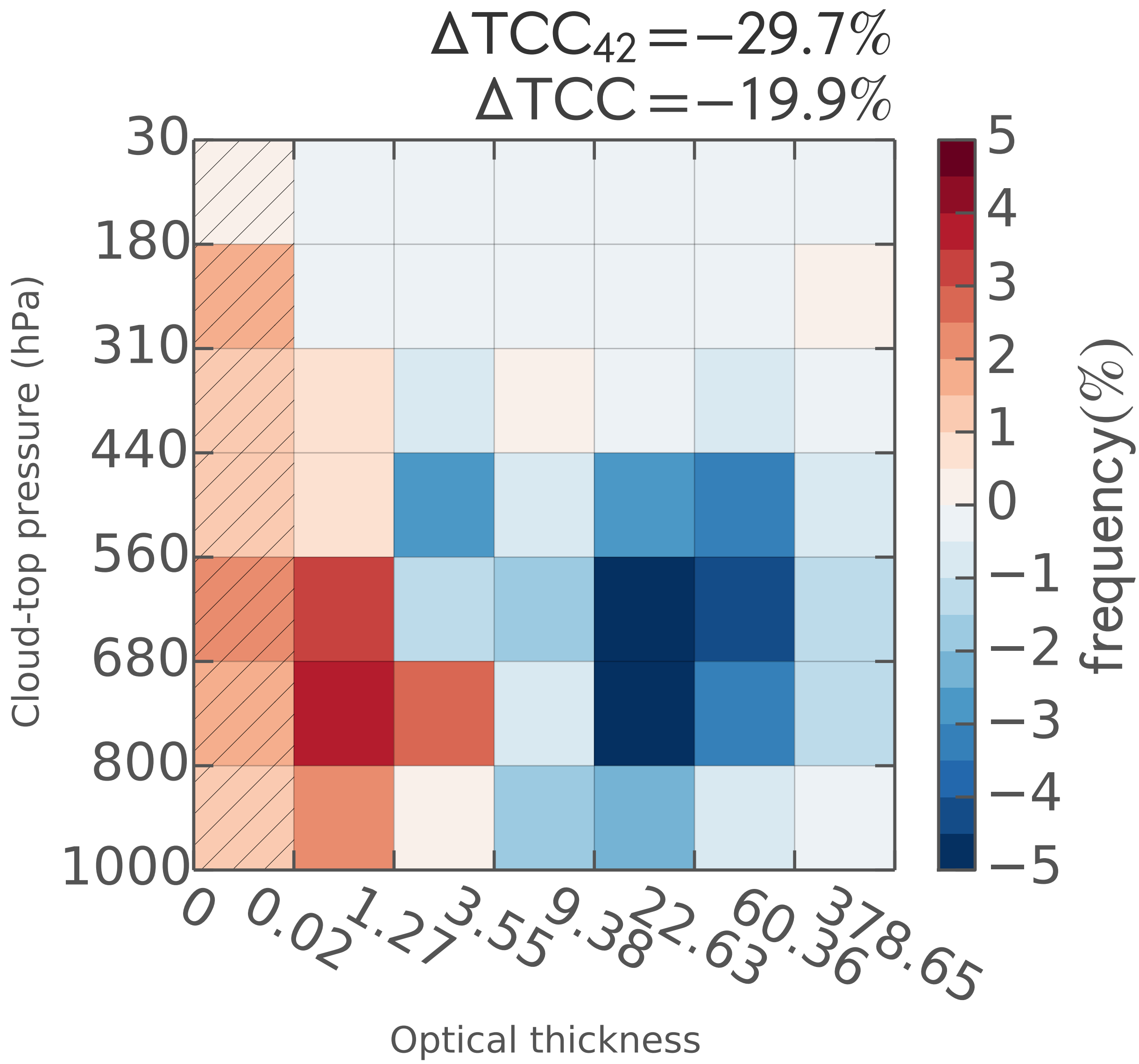

Fig. 2. The mean cloud bias (ACCESS1.3−ISCCP) over the region of interest for two austral summers (DJF), presented as the difference between CTP-τ joint histograms. The part of the histogram representing sub-visible optical thicknesses ($\tau < 0.3$), which is simulated in ACCESS1.3 but not observed in ISCCP, is hatched. At top-right the total cloud cover (TCC) error is indicated for the full joint histogram and for the visible (42-element) joint histogram.

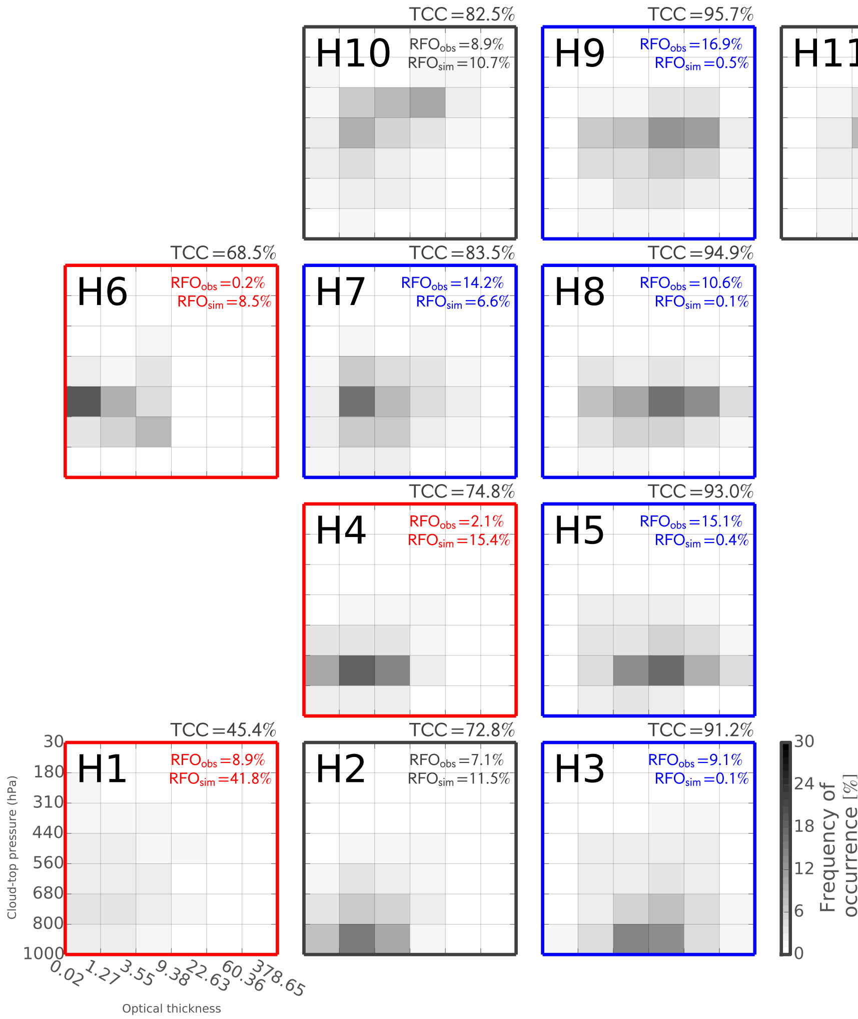

FIG. 3. The CTP-τ joint histograms representing the cluster centroids of the hybrid cloud regimes. The hybrid cloud regimes are arranged according to the dominant features of the joint histograms with the optically thinnest and lowest cloud regime in the bottom-left, and the optically-thickest and highest cloud regime in the top-right such that clouds of similar cloud-top pressures are comparably along the horizontal axis, and similar optical thicknesses along the vertical axis. The mean observed and simulated RFO over the regions of interest are indicated in the top-right corner of each histogram. Where the cloud regime is under (over)-represented in ACCESS1.3 by more than 50 % with respect to the observed value, the histogram is bordered in blue (red). The total cloud cover for each cloud regime (TCC; the sum of each joint histogram) is indicated at top-right.

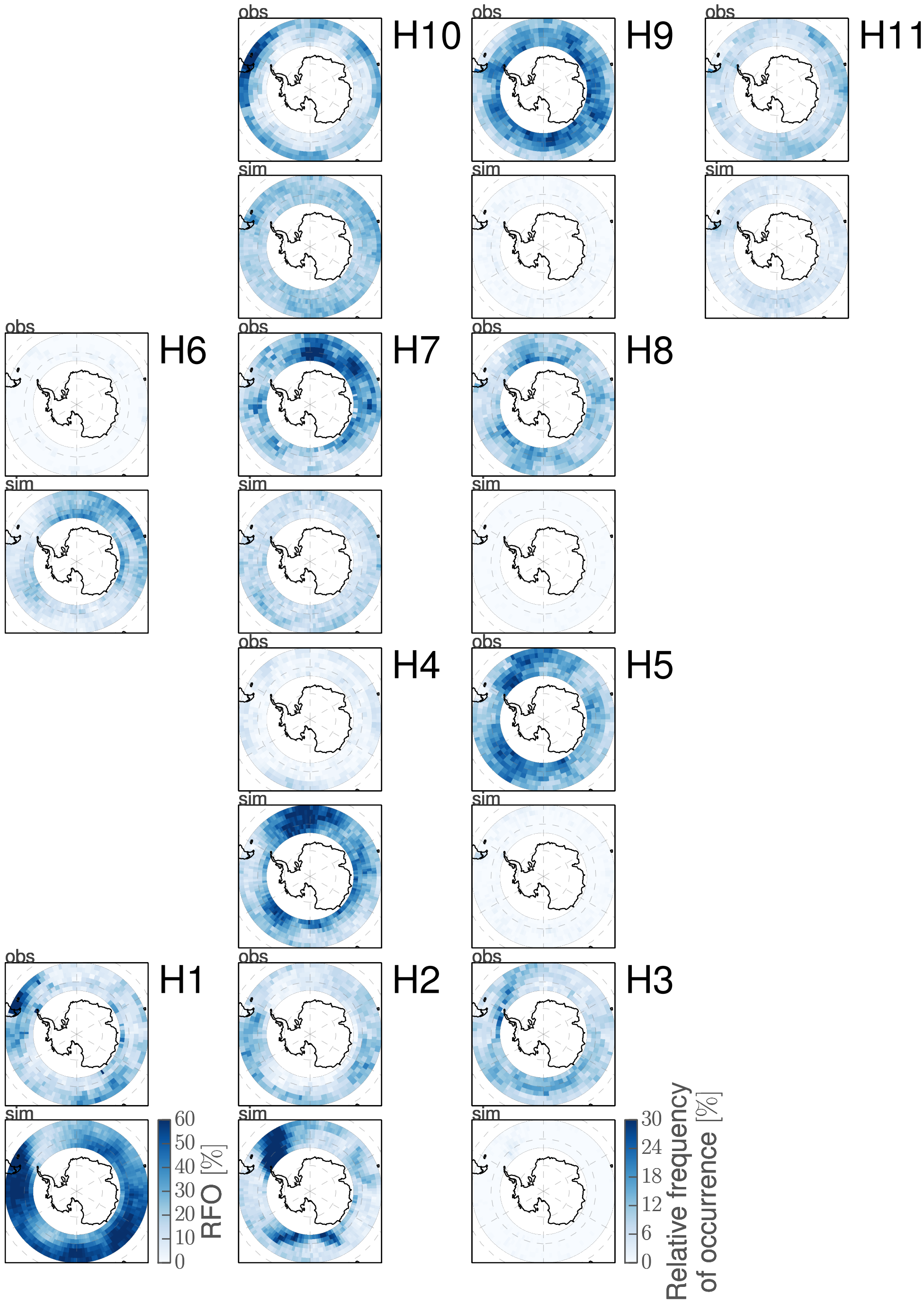

Fig. 4. Maps of the observed and simulated RFO of the hybrid cloud regimes over the region of interest. As in Figure 3, the hybrid cloud regimes are arranged according to the dominant features of the CTP-τ histogram, with the optically thinnest and lowest regime in the bottom-left and the optically thickest and highest cloud regime in the top-right. Note that the simulated RFO of H1 is on a different color scale to resolve the significant overproduction of this hybrid cloud regime in ACCESS1.3.

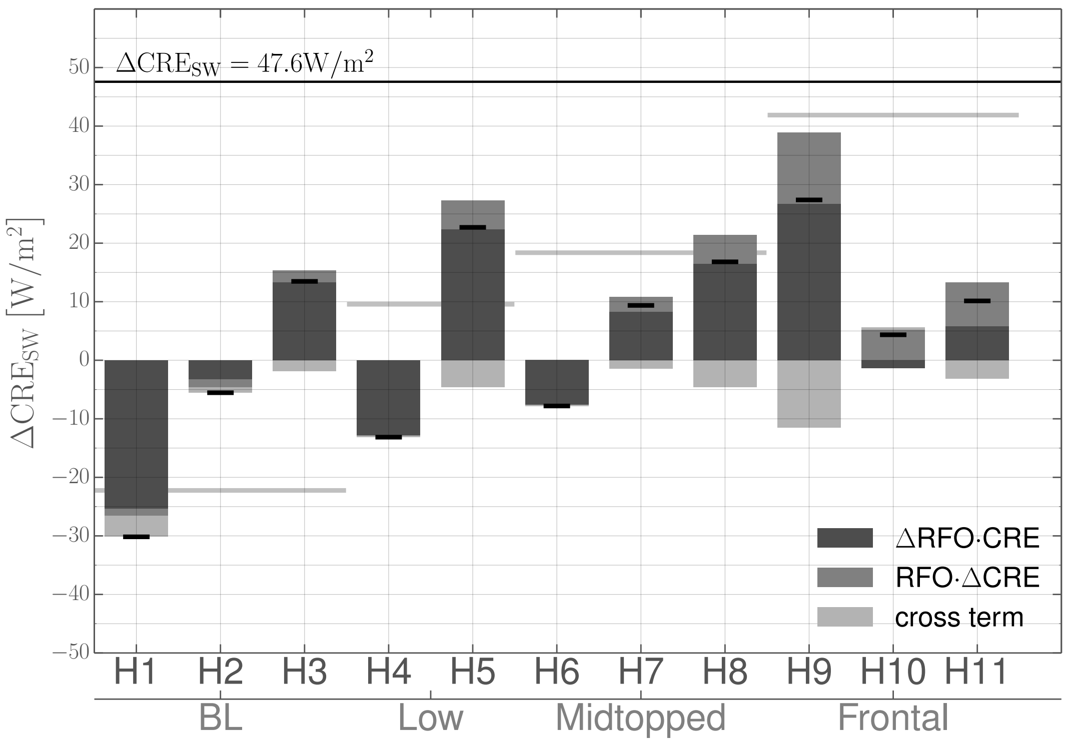

FIG. 5. The $\mathrm{CRE_{SW}}$ bias in ACCESS1.3 with respect to ISCCP FD radiative flux observations. The biases are decomposed into parts related to errors in RFO and $\mathrm{CRE_{SW}}$, and a cross-term. Black bars indicate the total $\mathrm{CRE_{SW}}$ bias associated with each cloud regime, and the total mean bias over the region of interest is indicated with a thick black line. Very pale bars indicate the net contribution to the $\mathrm{CRE_{SW}}$ error across each CTP-level class.

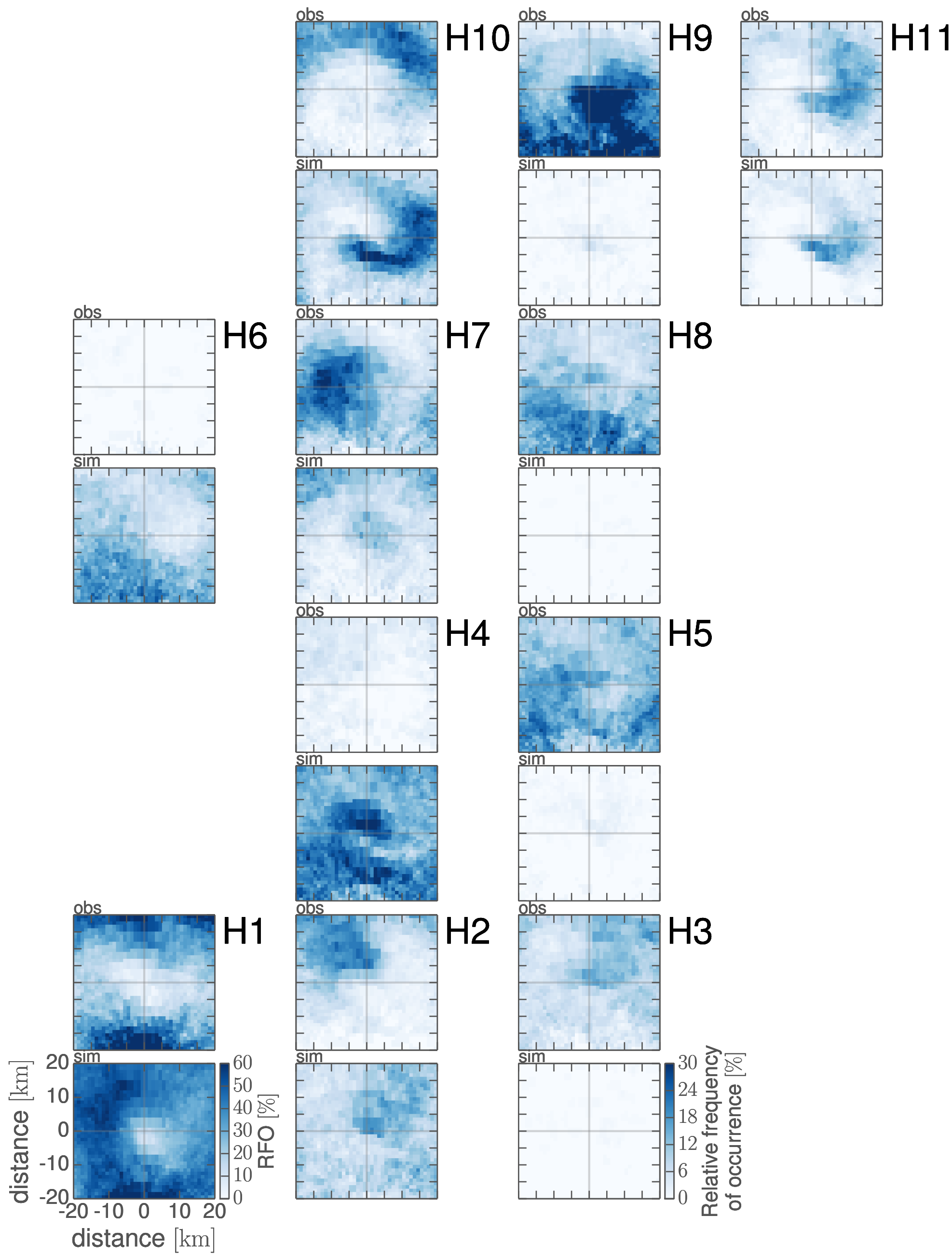

Fig. 6. Observed (above) and simulated (below) relative frequency of occurrence (RFO) of each hybrid cloud regime in the context of the composite extratropical cyclone. The cloud regimes are organized according to optical thickness (horizontal axis) and cloud top pressure (vertical axis). Note that the simulated RFO of H1 is on a different color scale to resolve the significant over-production of this hybrid cloud regime in ACCESS1.3.

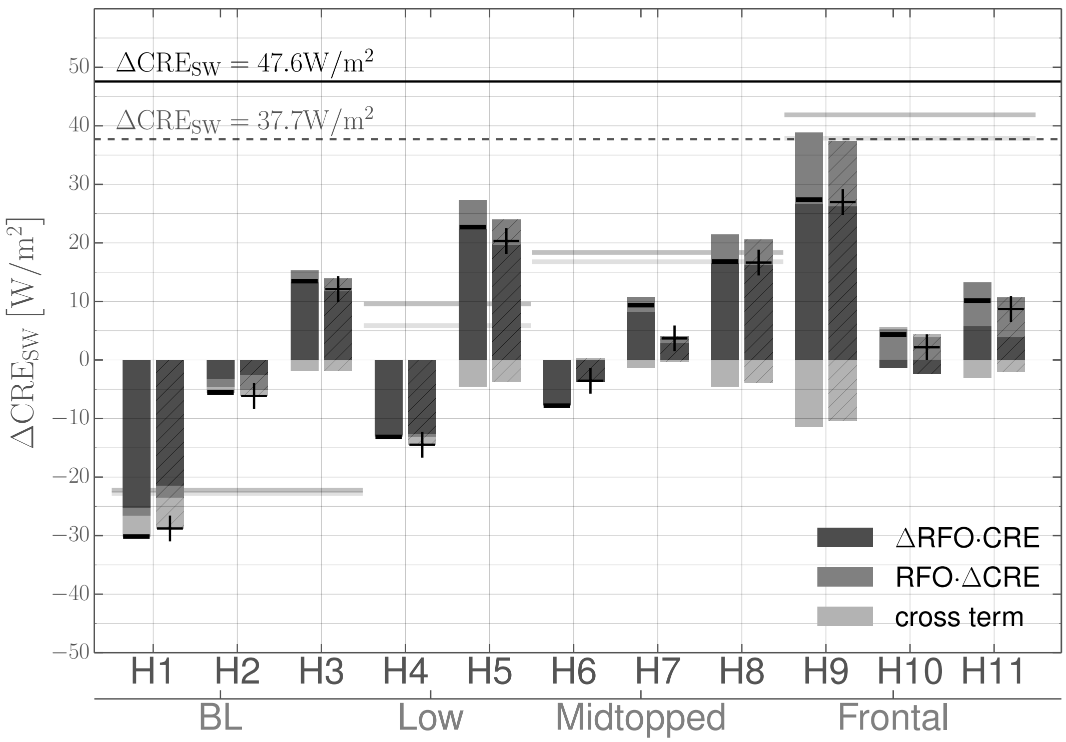

FIG. 7. A comparison of the decomposed SW biases associated with the modified microphysics and the control simulation. The hatched bars relate to the modified microphysics case. Solid bars (crosses) indicate the total CRE_{SW} bias associated with each cloud regime in the original (modified) model. Pale and very pale bars indicate the combined contribution to the CRE_{SW} error across each CTP-level class in the original and modified cloud microphysics parameterizations.